PFC/JA-85-5

Soft X-ray Tomography on Alcator C

R. S. Granetz and J. F. Camacho

Plasma Fusion Center
Massachusetts Institute of Technology
Cambridge, MA 02139

January 1985

This work was supported by the U.S. Department of Energy Contract No. DE-AC02-78ET51013. Reproduction, translation, publication, use and disposal, in whole or in part by or for the United States government is permitted.

Soft X-ray Tomography on Alcator C

R.S. Granetz and J.F. Camacho

Abstract

Using 80 miniature soft x-ray detectors viewing along chords through a plasma cross-section at one toroidal location, tomographic reconstructions of emissivity have been obtained without the need for assuming any symmetry or rotation of the plasma. In one class of plasma discharges, it is found that a large $m = 1$ oscillation, which previously had been ascribed to the rotation of an MHD instability, actually is not rotating at all.

Soft x-ray arrays are routinely used on tokamaks to look at MHD phenomena such as sawtoothing, the $m = 1$ precursor oscillation, $m \geq 2$ instabilities, as well as plasma position, impurity radiation, etc. Detailed analyses of the x-ray signals using techniques of x-ray tomography have been done by several experimenters [1-5] to obtain a 2-dimensional reconstruction of the emissivity function, $\varepsilon(r, \theta)$. Typically however, the number and arrangement of detector views which are available does not provide sufficient information to yield a useful image unless some simplifying assumptions are made. One common technique is to assume the x-ray emissivity has a specified functional form which includes one or more adjustable parameters [2]. In this case, reconstructing an image consists of finding the values of the free parameters which best reproduces the original signals. In situations where there are a very limited number of viewing chords, only very simple functional forms with one or two adjustable parameters can be used.

Another technique, which is widely used when studying MHD instabilities, is to assume the oscillations typically seen on the x-ray signals are due to a perturbation in the emissivity which is rotating with a known time behavior (not necessarily sinusoidal) [3,4,5]. This enables the "generation" of extra signals from angles at which there are no detectors, since rotation provides a direct correlation between measured signals versus time at a given angle and unmeasured signals at any other angle. This assumption is valid if the emission pattern

is rotating rigidly and not changing amplitude during one oscillation period. Although researchers worry about whether or not these conditions are met in actual measurements, there has been very little questioning of the fundamental assumption made here, namely that rotation causes the oscillations in the x-ray signals.

In order to generate tomographic reconstructions without any of the above assumptions, it is necessary to have signals from line chords at many different angles, ϕ, and impact radii, p. Figure 1 shows the definition of p and ϕ for one chord. These two parameters uniquely identify each detector view. Ideally one would want to have chords approximately equally spaced in both p and ϕ. The finite number of detectors, and therefore p and ϕ values, puts limits on the spatial resolution in the radial and angular directions respectively. This is true regardless of the mathematical algorithm used to do the reconstruction. On Alcator C we have installed an 80-channel array of miniature solid-state soft x-ray detectors arranged in ten fans, each fan having 8 chords, all at one toroidal location [6]. Due to the limited access available on this tokamak, the detector fans are not equally spaced in angle; rather they are bunched towards the top and bottom of the plasma cross-section as shown in the skematic in Fig 2. The lack of views in the horizontal direction leaves angular gaps in (p, ϕ) space and therefore limits the poloidal resolution. Although the 80 detector locations are clearly not optimum, there is still enough information to do tomographic reconstructions of some detail *without any of the above assumptions*, even allowing for realistic errors in detector calibration and positioning.

After careful evaluation of several different mathematical techniques for reconstructing the 2-dimensional emission function, we have found that an analytic solution due to Cormack [7,8] yields the best results with our experimental setup. Given that no emission exists outside a certain radius (which in Alcator is $\sim$10 - 11 cm, where a = 16.5 cm), the x-ray signals may be approximated as line integrals as long as the widths of the viewing chords are much narrower than the spatial variation of the emissivity:

$$f(p,\phi) = \int_{L(p,\phi)} g(r,\theta)\, dL \qquad (1)$$

where $f(p,\phi)$ is the x-ray brightness (Watts/cm^2/steradian) measured by the detector viewing along the chord, L, defined by p and ϕ and $g(r,\theta)$ is the soft x-ray emissivity

(Watts/cm^3). This is true as long as the plasma is optically thin in the x-ray spectral region. Tomography consists of inverting equation (1) for $g(r,\theta)$, which is a two-dimensional problem. As a first step this can be transformed into a set of one-dimensional equations by expanding in Fourier harmonics in angle. Let:

$$g(r,\theta) = \sum_{m=0}^{\infty} [g_m^c(r)\cos m\theta + g_m^s(r)\sin m\theta] \tag{2}$$

$$\text{and} \quad f(p,\phi) = \sum_{m=0}^{\infty} [f_m^c(p)\cos m\phi + f_m^s(p)\sin m\phi] \tag{3}$$

Then equation (1) becomes:

$$f_m^{c,s}(p) = 2\int_p^1 \frac{g_m^{c,s}(r)\,T_m(p/r)\,r}{(r^2-p^2)^{1/2}}\,dp \tag{4}$$

where $T_m(x) = \cos(m\cos^{-1}x)$ is a Tschebycheff polynomial. This representation is quite useful in reconstructing the emission from a tokamak plasma because MHD theory predicts that only the lowest angular harmonics are involved in the equilibrium and principal instabilities.

Cormack [7] proved the solution to equation (4) is:

$$g_m^{c,s}(r) = -\frac{1}{\pi}\frac{d}{dr}\int_r^1 \frac{r f_m^{c,s}(p)\,T_m(p/r)}{(p^2-r^2)^{1/2}p}\,dp \tag{5}$$

For the $m = 0$ component, this reduces to the familiar Abel inversion. Unfortunately, the direct numerical application of equation (5) is noise sensitive because of the differentiation involved and is therefore of limited use with real data. To overcome this problem, Cormack [8] found a special pair of expansion polynomials which satisfy equation (5). If $f_m(p)$ is expanded as follows:

$$f_m(p) = 2\sum_{l=0}^{\infty} a_{ml}\sin[(m+2l+1)\cos^{-1}p] \tag{6}$$

then

$$g_m(r) = \sum_{l=0}^{\infty}(m+2l+1)\,a_{ml}R_{ml}(r) \tag{7}$$

where

$$R_{ml}(r) = \sum_{s=0}^{l} \frac{(-1)^s (m + 2l - s)!\, r^{m+2l-2s}}{s!\,(m + l - s)!\,(l - s)!}$$

are called the Zernicke polynomials. The coefficients, a_{ml}, are found by doing a least squares fit of eq. (6) to the data and thus this method is relatively insensitive to noise. In addition, the special expansion functions for $f_m(p)$ satisfy certain mathematical constraints having to do with the number of radial nodes in the projections, which further reduces the effects of noise in the data. In practice, we find that the detector configuration on Alcator C allows for reconstructions having angular harmonics $m = 0$ and 1, and radial harmonics $l = 0$ to 6. (The addition of side arrays in the near future will permit the reconstructions to include up to $m = 2$.) These limits are determined by an error analysis which takes account of the fact that the viewing geometry and detector calibrations have both random and systematic errors which will degrade the reconstructions. Starting with a reasonable test emission function, we calculate the flux to each detector assuming a systematic error ($\sigma = 0.5$ mm) in detector position as well as additional random noise due to calibration inaccuracies ($\sigma = 3\%$). The tomographic reconstruction of these pseudo-signals is then compared to the test function. We find that the m and l harmonic numbers must be restricted to the previously specified values in order to reliably reproduce the input.

Three examples of x-ray tomography of Alcator plasmas will be exhibited. The first is from a typical sawtoothing plasma (Fig. 3). The pair of reconstructions in Figs. 4 and 5 show the change in the emissivity which occurs at the crash of a sawtooth. It should be emphasized that since only a finite number of harmonics are used, there is a residual "ripple" noise in the reconstructions which is of order $\sim 5\%$. Therefore the slight hollowing in the 3-D plot after the crash may or may not be real. However the general flattening of the center and broadening of the outer regions is resolvable. Note also that the $m = 1$ component evident in Fig. 4 is due to an outward shift of the equilibrium with respect to the center of the vacuum vessel and not an $m = 1/n = 1$ instability. (The tomography algorithm makes no a priori assumption of plasma center position.)

The second example is from a pellet-fueled sawtoothing plasma which exhibits large $m = 1$ "precursor" oscillations immediately before each sawtooth crash (Fig. 6). This

instability is believed to be a resistive tearing mode which forms a magnetic island and grows until it eventually causes the sawtooth crash [9,10,11]. The reason for the oscillatory nature of the x-ray perturbations has always been ascribed to island rotation, either due to ω_* diamagnetic effects (the so-called drift tearing mode [12]) or to radial electric fields giving rise to an $\vec{E} \times \vec{B}$ drift.

In Fig. 7 the reconstructions from an oscillation cycle are shown. By following the peak of the emission from frame to frame, it is seen that the perturbation does indeed exhibit an apparent rotation in the electron diamagnetic direction, although it is not exactly sinusoidal. In frames 7*c* and *e* there is a flattened region near the $q = 1$ surface which could conceivably be the center of a magnetic island. However this feature is not apparent in the other frames and we do not understand why this is so. It may be that the perturbation changes shape as it rotates from high-field to low-field regions.

A final example of tomography on Alcator is from a lower current pellet-fueled plasma that is not sawtoothing but which does exhibit large $m = 1$ oscillations on the soft x-ray signals (Fig. 8). As in the previous example, this behavior seems to indicate mode rotation. However, the x-ray reconstructions over one cycle, which are displayed in Fig. 9, show that there is *no rotation* associated with these oscillations. Instead an instability seems to grow and to compress the plasma on the inner major radius side. Then within 100 μsec (frame 9*e* to 9*f*) the mode disappears and the x-ray emissivity returns to its normal circular shape. This process repeats itself over and over again, resulting in the oscillating pattern on the individual soft x-ray signals. We have made computer movie films of thousands of frames of the tomography data and they help to elucidate this motion and clearly show the difference between this type of discharge and a sawtoothing discharge.

What causes the difference in the rotation behavior of these two types of discharges? There is no drastic difference in the pressure gradient and therefore any rotation due to ω_* effects would remain approximately unchanged. This leads one to postulate that a radial electric field may be contributing to the mode rotation and that substantial differences in E_r may lead to the different rotation behavior. This change in electric field would be expected to affect the radial impurity transport, among other things, and this is indeed seen. In Alcator, non-sawtoothing plasmas have a relatively higher soft x-ray flux than

sawtoothing discharges, presumably due to enhanced impurity radiation. In addition there are indications that the impurity confinement time in Alcator, which is normally finite, may approach infinity in non-sawtoothing plasmas [13]. In other words, impurities may actually accumulate on axis.

In summary, using 80 soft x-ray detectors at one toroidal location, we have obtained tomographic reconstructions of the x-ray emissivity without assuming any symmetry or rotation of the plasma. We find both rotating and non-rotating instabilities—the non-rotating oscillations are caused by the rapid and repetitive growth and decay (reconnection?) of an $m = 1$ mode rather than the rotation of a saturated, steady-state island. This leads us to postulate that there is a change in the radial electric field, which in turn affects the nature of impurity confinement and possibly other plasma properties as well. Future work includes the addition of several side arrays to enable higher Fourier poloidal harmonics to be included in the reconstructions. In addition, by injecting various impurities into the plasma we plan to accurately measure the differences in impurity confinement between rotating and non-rotating discharges.

REFERENCES

[1] V.K. PARÉ, J.D. BELL, A.P. NAVARRO, J.L. DUNLAP, E.T. BLAIR, "MHD Mode Structure and Rotation as Shown by Soft X-ray Imaging in ISX-B," Bull. Am. Phys. Soc. **28** (1983) 1254.

[2] G. JAHNS, R. MOORE, H. ST. JOHN, R. STOCKDALE, R. SNIDER, "Internal Geometry of Doublet III Discharges," Bull. Am. Phys. Soc. **29** (1984) 1363.

[3] P. SMEULDERS, Nucl. Fusion **23** (1983) 529.

[4] N.R. SAUTHOFF, S. VON GOELER, W. STODIEK, Nucl. Fusion **18** (1978) 1445.

[5] Y. NAGAYAMA, S. TSUJI, K. KAWAHATA, N. NODA, S. TANAHASHI, Jpn. J. Appl. Phys.. **20** (1981) L779.

[6] J.F. CAMACHO AND R.S. GRANETZ, "Soft X-ray Tomography Results from Alcator C," Bull. Am. Phys. Soc. **29** (1984) 1224.

[7] A.M. CORMACK, J. Appl. Phys. **34** (1963) 2722.

[8] A.M. CORMACK, J. Appl. Phys. **35** (1964) 2908.

[9] B.B. KADOMTSEV, Sov. J. Plasma Phys. **1** (1975) 389.

[10] M.A. DUBOIS, A.L. PECQUET, C. REVERDIN, Nucl. Fusion **23** (1983) 147.

[11] G.L. JAHNS, M. SOLER, B.V. WADDELL, J.D. CALLEN, H.R. HICKS, Nucl. Fusion **18** (1978) 609.

[12] D. BISKAMP, Nucl. Fusion **19** (1979) 777.

[13] J.L. TERRY, E.S. MARMAR, M.J. GREENWALD, J. PARKER, "Observation of Change in Molybdenum Transport after a Large Density Increase from Pellet Injection," Bull. Am. Phys. Soc. **28** (1983) 1164.

List of Figure Captions

Figure 1 — Definition of the chord impact parameter, p, and the chord angle, ϕ. Note that p is usually normalized to the range 0–1. The emitting region must be confined to $p < 1$ for the algorithm described in this paper.

Figure 2 — Illustration of the 80 different viewing chords of the Alcator tomography experiment. The system is configured in 10 "fans", each fan having 8 individual detectors.

Figure 3 — X-ray sawteeth from a typical Alcator plasma. Tomographic reconstructions are done at the indicated times to compare the x-ray emissivity before and after a sawtooth crash.

Figure 4 — The magnitude of the $m = 0$ and $m = 1$ components of emissivity versus radius before (solid) and after (dashed) a sawtooth crash. The emissive power has not been corrected for the effects of our beryllium filter windows.

Figure 5 — 3-D plots of the x-ray emissivity before and after a sawtooth crash.

Figure 6 — An x-ray signal from a pellet-fueled plasma showing large sawteeth and $m = 1$ precursor oscillations. Several reconstructions, which span the indicated cycle of precursor oscillation, are presented in the following figure.

Figure 7 — Contour plots of x-ray emissivity which show a rotating perturbation at a radius of approximately 4 cm.

Figure 8 — An x-ray signal from another pellet-fueled plasma showing large oscillations but no sawteeth. Several reconstructions, which span the indicated single cycle of oscillation, are presented in the following figure.

Figure 9 — Contour plots of x-ray emissivity show a growing perturbation (location indicated by arrows) which appears to compress and push the plasma, but which does not rotate.

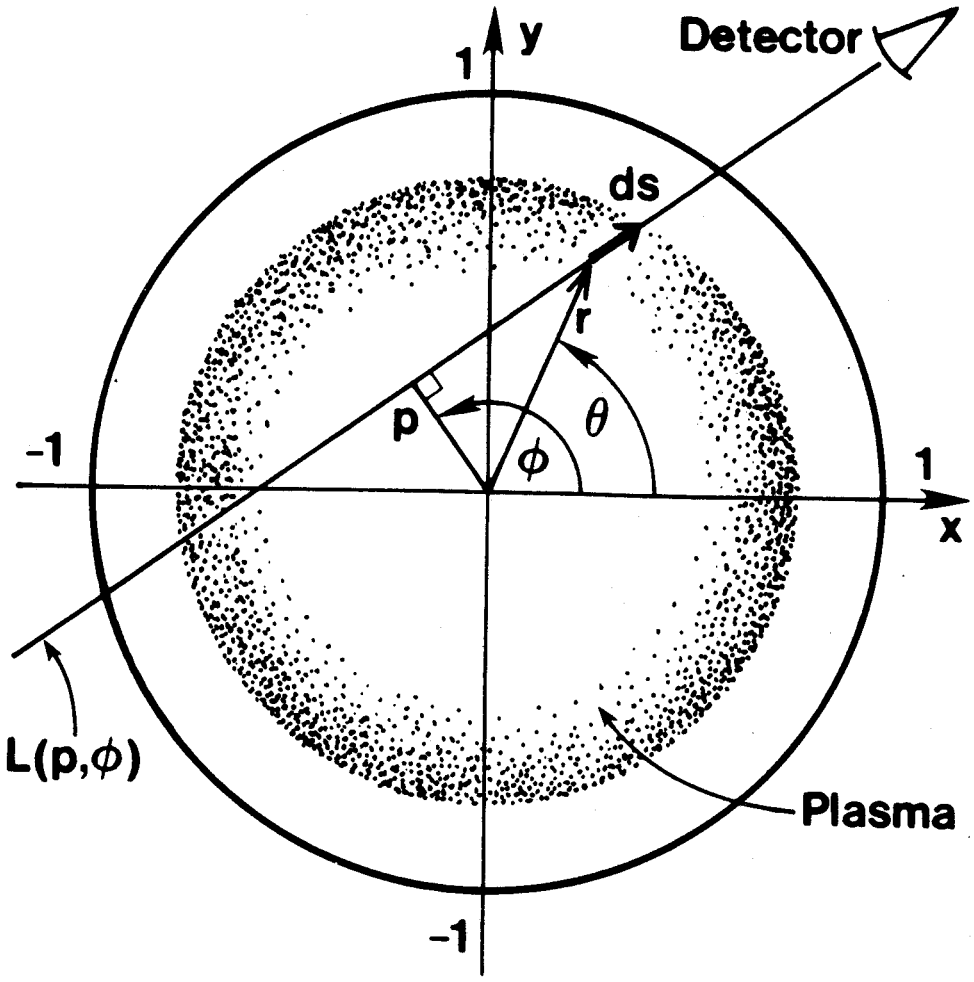

FIGURE 1

8608/7/4

L/L/8098

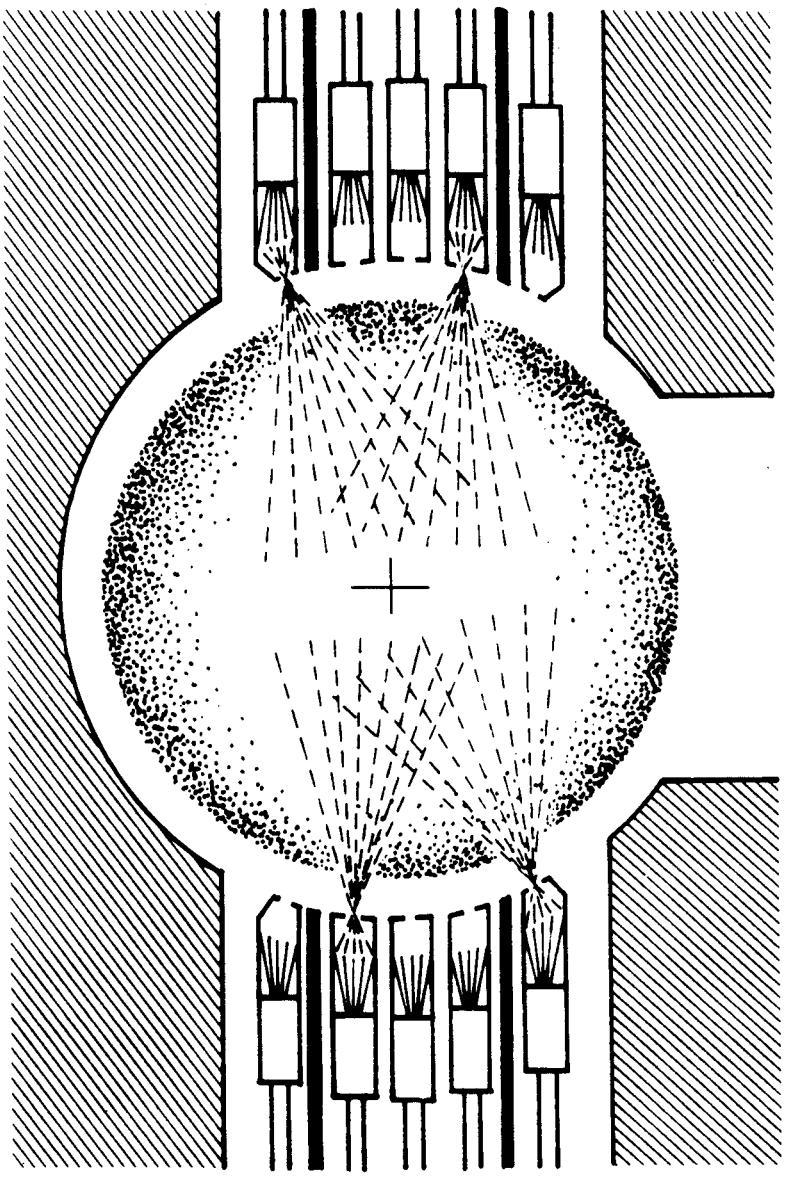

FIGURE 2

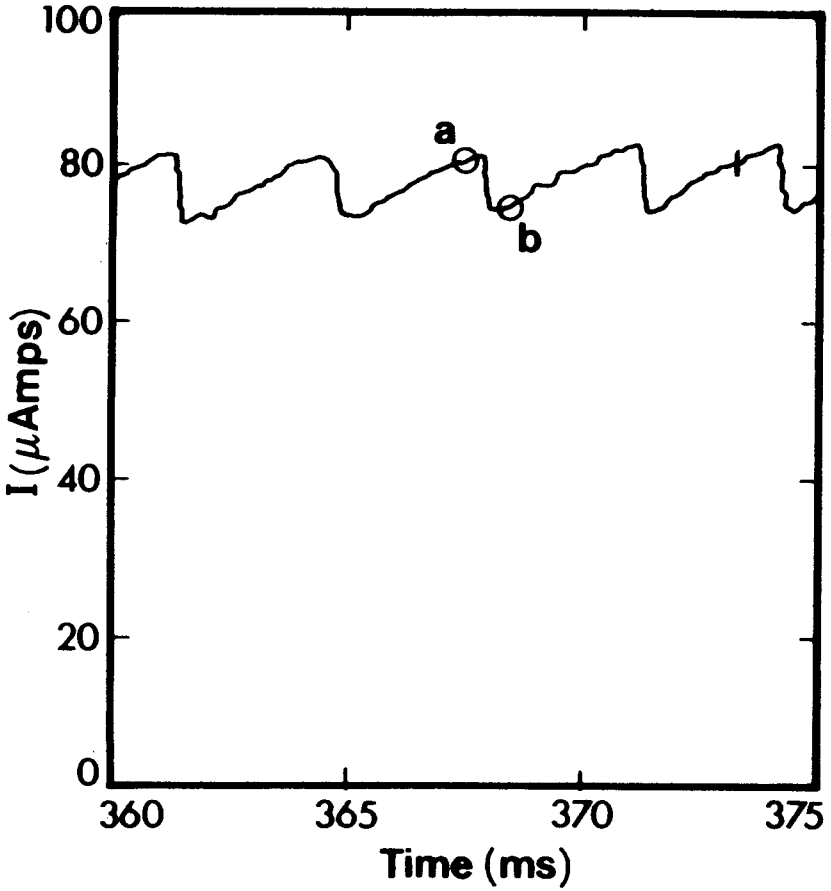

FIGURE 3

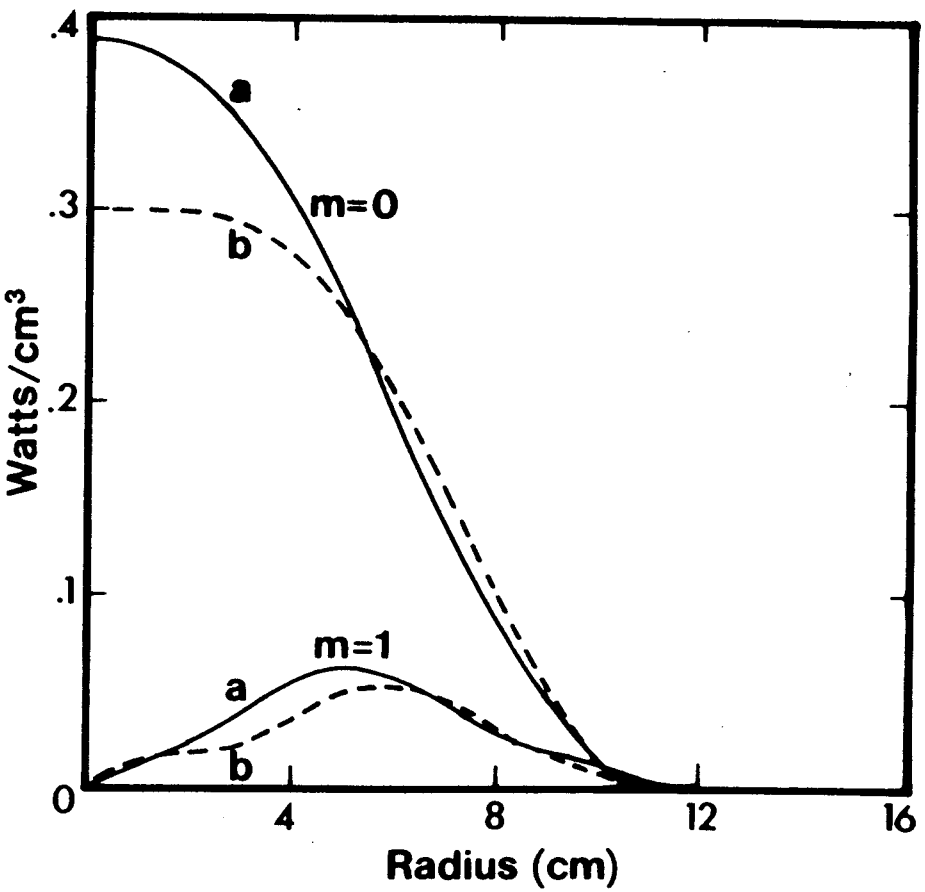

FIGURE 4

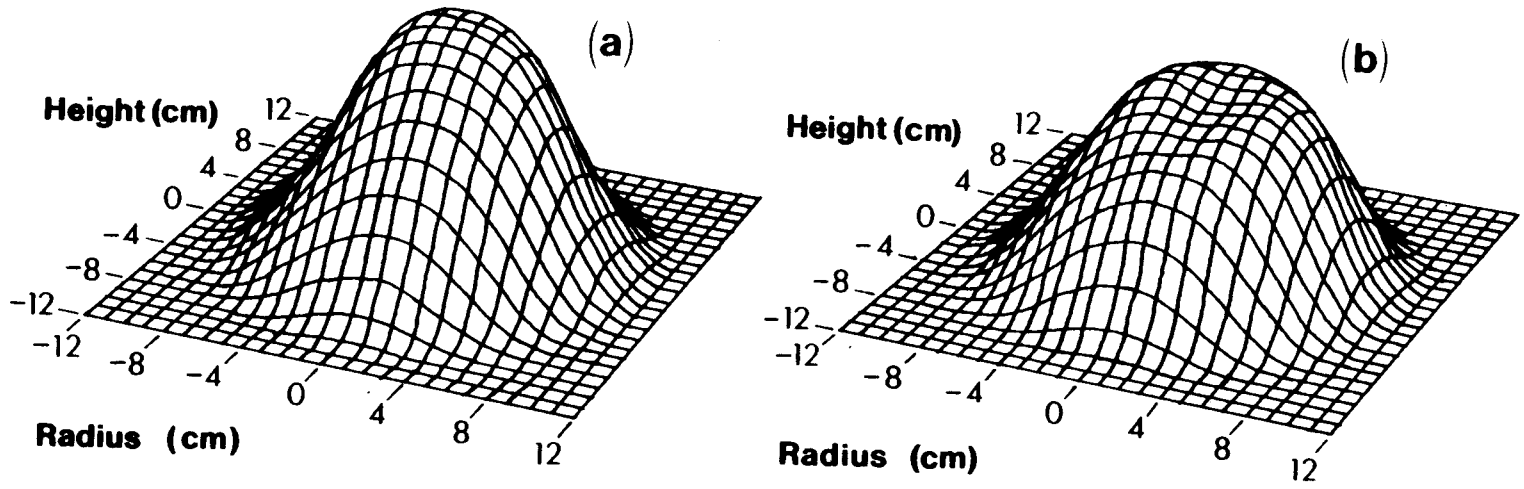

FIGURE 5

8608/7/2

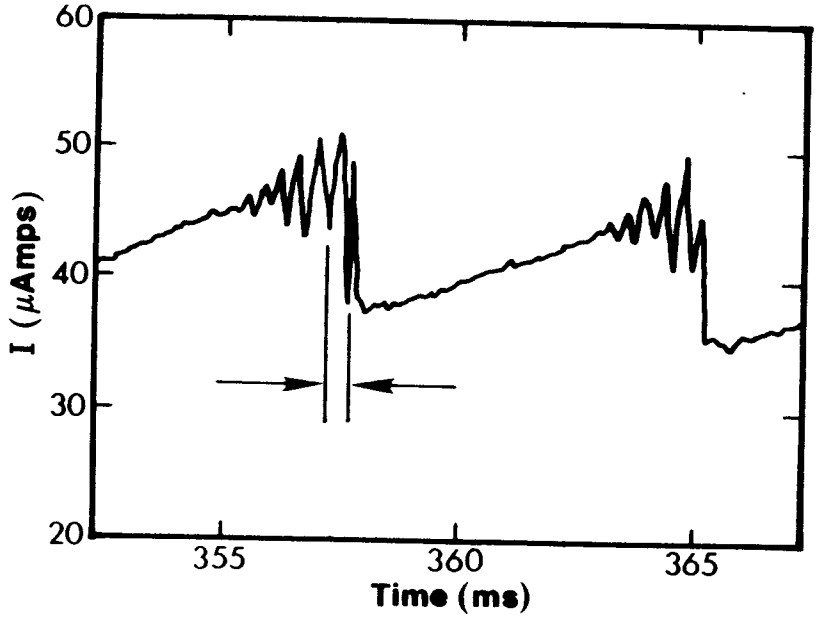

FIGURE 6

B608/7/34

8608/73a

FIGURE 7

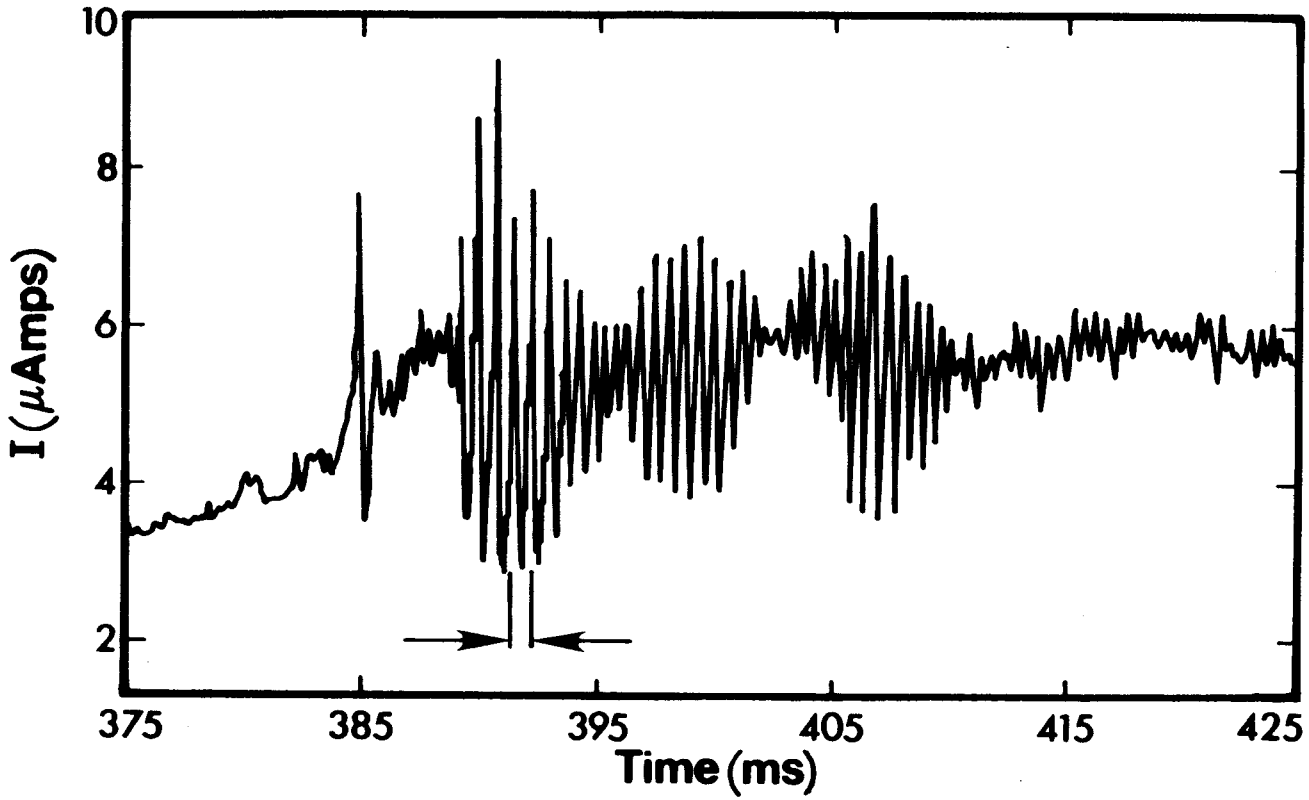

FIGURE 8

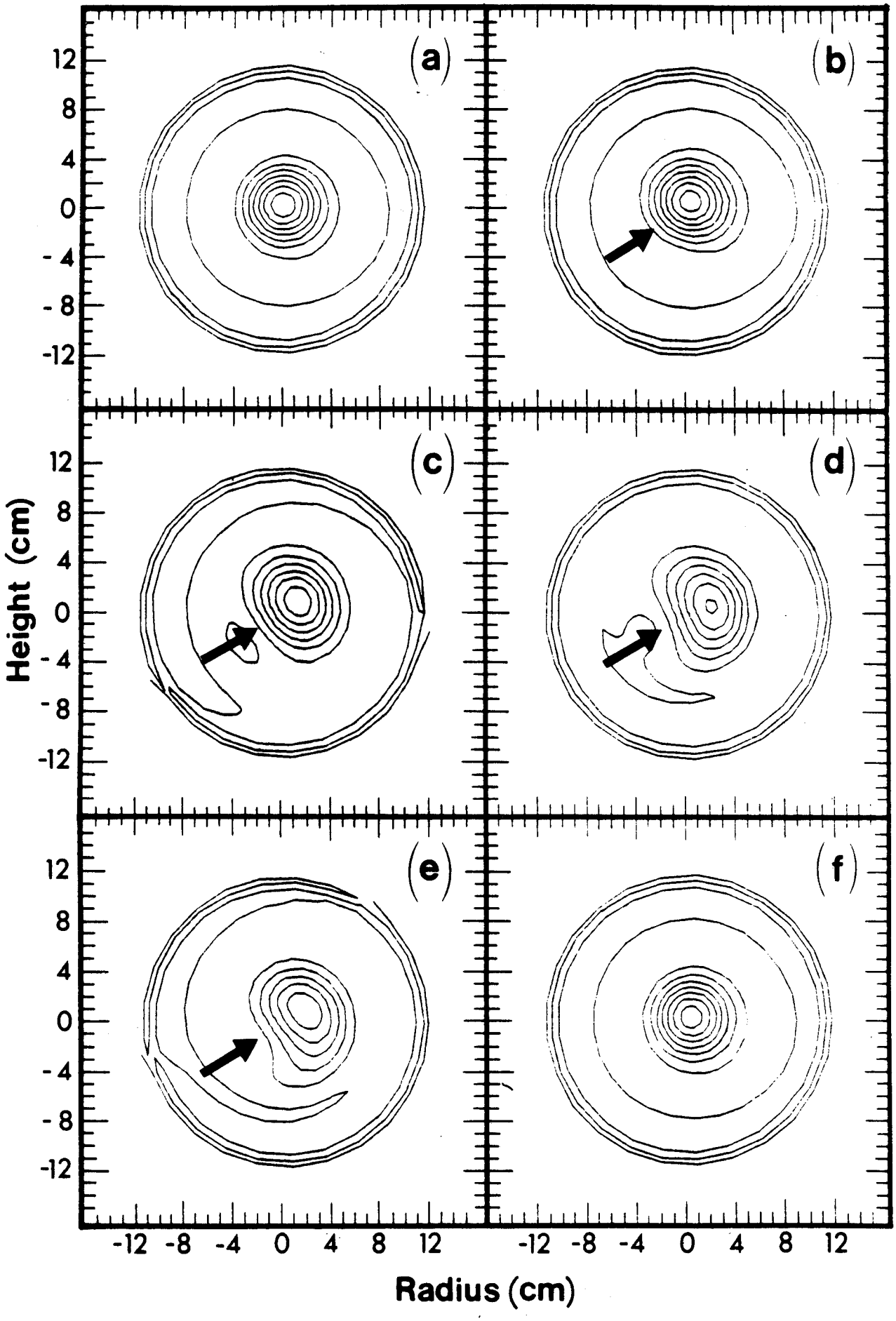

FIGURE 9

8608/7.5